Development of an Automated Roughness Estimation Algorithm for Sidescan Imagery

Maura C. Lohrenz and Marlin L. Gendron

Abstract— **Estimations of seafloor clutter (also called mine-like echoes) and roughness (bottom relief) are needed during mine warfare operations to determine seafloor type for a geographic region of interest. Analysts at the Naval Oceanographic Office estimate bottom clutter and roughness from sidescan sonar imagery (SSI). However, detecting clutter and determining roughness manually is often time consuming and can produce inconsistent results. The Naval Research Laboratory has developed an algorithm to automatically derive seafloor roughness from SSI. In repeated trials, results of the automated roughness algorithm correlated well (as high as 87%) with manual roughness estimations.**

Index Terms—**Acoustic signal detection, Computer-aided analysis, and Sonar signal processing.**

I. Introduction

MODERN remote sensing devices are capable of collecting tremendous amounts of high-resolution digital imagery in remote locations. This imagery must be evaluated by an analyst to obtain useful information (e.g., detect and identify specific features of interest). If the imagery is time-critical, analysis must be performed as quickly as possible. However, the sheer volume of data available to analysts often precludes timely analysis [1], [2].

The design and development of computer-aided detection algorithms has advanced significantly in the past few decades in many fields, such as medicine. In 1967, the difficulty of viewing and analyzing large amounts of data in screening mammograms was recognized, and computer-aided image analysis algorithms were suggested [3]. There were also early attempts to identify lesions such as malignant tumors using detection algorithms [4]. It was suggested that such algorithms should be incorporated into all new medical digital imaging systems [5].

Another field that has benefited from automated detection algorithms is Mine Warfare (MIW). Estimations of bottom clutter (also called mine-like echoes) and roughness (bottom relief) are two of the components needed during MIW operations to determine the seafloor type for a geographic area. Analysts at the Naval Oceanographic Office (NAVOCEANO) obtain bottom clutter and roughness estimations for MIW directly from sidescan sonar imagery (SSI). Detecting clutter and determining roughness manually can be time consuming and often produce inconsistent results, due to the subjective nature of the analysis. Automated algorithms can potentially derive clutter and roughness from SSI in a more consistent and timely manner.

Features such as pockmarks, sand ripples, and rocks on the seafloor are visible in SSI as bright spots ("brights") with adjacent shadows. The Naval Research Laboratory (NRL) developed a real-time clutter detection algorithm (transitioned to NAVOCEANO in 2001) that quickly and reliably identifies clutter in SSI and clusters the results into polygons. An object's height (estimated from the length of its shadow) is one measurement used to determine whether the object is mine-like. The authors theorized that height also could be used to automatically estimate seafloor roughness.

NRL recently developed a new automated roughness estimation algorithm, based on the clutter detection algorithm, to automatically derive seafloor roughness from SSI. The roughness algorithm was transitioned to NAVOCEANO in 2006. This paper provides an overview of the clutter detection algorithm, describes the roughness algorithm, and presents test results and comparisons with manual roughness estimations.

II. Clutter Detection Algorithm

A. Overview

The real-time clutter detection algorithm developed by the authors ingests one scan line of SSI at a time. Across-track bright and shadow positions, lengths, and intensity information are immediately gathered from the scan line and stored in two one-dimensional geospatial bitmaps (GBs): one each for shadows and brights. A circular lookup table is created to "window" the imagery several scan lines at a time. This lookup table is the same width as the GBs and is populated with the positions and run-lengths of shadows and brights stored in the GBs. The window is used to make the final detection decision.

B. Geospatial Bitmaps (GBs)

Due to real-time processing considerations, the authors' algorithm relies on a patented GB technique [6]. Simple

Manuscript received January 19, 2007. This work was sponsored under Program Element 602435N by the Naval Research Laboratory (NRL) 6.2 Base Program.

Maura C. Lohrenz is with NRL, Stennis Space Center, MS 39529 USA (phone: 228-688-4611; fax: 688-4853; e-mail: mlohrenz@nrlssc.navy.mil).

Marlin L. Gendron is with NRL, Stennis Space Center, MS 39529 USA (e-mail: mgendron@ nrlssc.navy.mil).

Report Documentation Page

Form Approved
OMB No. 0704-0188

1. REPORT DATE	2. REPORT TYPE	3. DATES COVERED
JUN 2007		**00-00-2007 to 00-00-2007**

4. TITLE AND SUBTITLE	5a. CONTRACT NUMBER
Development of an Automated Roughness Estimation Algorithm for Sidescan Imagery	5b. GRANT NUMBER
	5c. PROGRAM ELEMENT NUMBER
6. AUTHOR(S)	5d. PROJECT NUMBER
	5e. TASK NUMBER
	5f. WORK UNIT NUMBER
7. PERFORMING ORGANIZATION NAME(S) AND ADDRESS(ES) **Naval Research Laboratory,1005 Balch Blvd,Stennis Space Center ,MS,39529**	8. PERFORMING ORGANIZATION REPORT NUMBER
9. SPONSORING/MONITORING AGENCY NAME(S) AND ADDRESS(ES)	10. SPONSOR/MONITOR'S ACRONYM(S)
	11. SPONSOR/MONITOR'S REPORT NUMBER(S)

12. DISTRIBUTION/AVAILABILITY STATEMENT
Approved for public release; distribution unlimited

13. SUPPLEMENTARY NOTES
Proceedings of the Oceans '07 Conference, Aberdeen, Scotland. June 18-21

14. ABSTRACT
see report

15. SUBJECT TERMS

16. SECURITY CLASSIFICATION OF:			17. LIMITATION OF ABSTRACT	18. NUMBER OF PAGES	19a. NAME OF RESPONSIBLE PERSON
a. REPORT **unclassified**	b. ABSTRACT **unclassified**	c. THIS PAGE **unclassified**	**Same as Report (SAR)**	**4**	

bitmaps, with a depth of one bit per pixel, are binary structures in which bits are turned on (set = 1) or off (cleared = 0). The index of each bit is unique and denotes its position relative to other bits in the bitmap. The author extended this concept to construct GBs in which every bit represents an object at some unique geospatial location. A set bit indicates that some object of interest exists (in this case a bright or shadow pixel) at that location, accurate to within the resolution of the bitmap. A cleared bit indicates the absence of any object at that location. Although a GB can be defined for an entire finite space, memory is only allocated (dynamically) when groups of spatially close bits are set, resulting in a compact data structure that supports very fast Boolean and morphological operations.

C. Pixel Intensity Thresholds

Across-track bright and shadow positions and lengths are stored in two GBs: one each for shadows and brights. Shadows and brights in a scan line are located by first adaptively obtaining a lower intensity threshold, i_{min}, such that all samples of intensity less than i_{min} are considered shadows. An upper intensity threshold, i_{max}, is set such that all samples of intensity above i_{max} are considered brights.

An appropriate gamma shift converts image intensities to fit a normal distribution, such that i_{min} and i_{max} are set to the quartiles of the shifted (normal) distribution. After i_{min} and i_{max} have been determined for scan lines with maximum intensity value > 128, the port and starboard halves of the scan lines are processed separately. Each half of the scan line can be represented by a vector, X, of length N. The following method is used to process shadows and brights for the starboard side; the port side is processed similarly.

Two GBs of size 1xN are created, one for shadows and one for brights. A different gamma adjustment, γ, based on an error approximation of the side-scan sonar parameters, is computed for position x within X, as shown in (1).

$$\gamma = e^{-\beta x / N} \tag{1}$$

β is based on the sonar parameters, such as time-varying gain. As β approaches infinity, the gamma correction approaches 0 over a greater range of X (Fig. 1), and therefore has less affect on intensity thresholds.

The bright and shadow thresholds $I_{min}(x)$ and $I_{max}(x)$ are defined in (2) and (3). All pixels with intensity values above $I_{max}(x)$ are considered brights, while all with intensities below $I_{min}(x)$ are considered shadows, and the corresponding bits in the bright and shadow GBs are set, as shown in Fig. 2.

$$I_{min}(x) = i_{min}(1- \gamma) \tag{2}$$
$$I_{max}(x) = i_{max}(1+ \gamma) \tag{3}$$

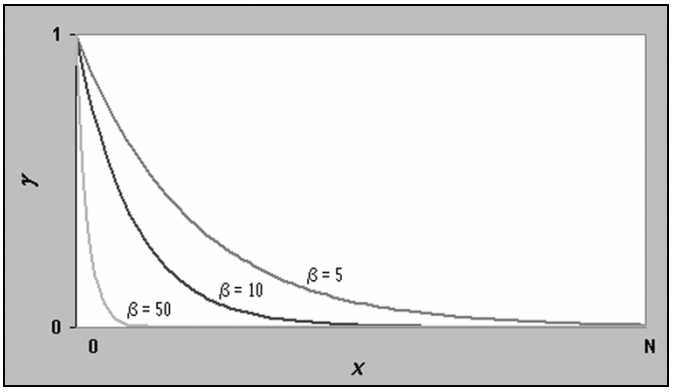

Fig. 1. Gamma as a function of β.

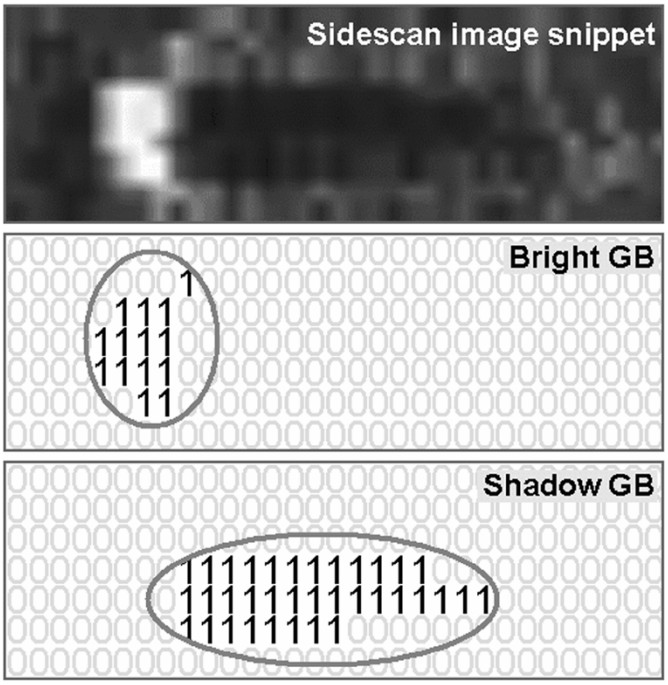

Fig. 2. GBs facilitate computer-aided detection of objects in SSI. Each row of bits in both GBs corresponds to a single scan line in the image. All pixels in the image with intensity greater than upper threshold I_{max} are considered "brights" and the appropriate bits in the bright GB are set. Likewise, all pixels in the image with intensity less than lower threshold I_{min} are considered "shadows" and the appropriate bits in the shadow GB are set.

Fig. 3 illustrates how the intensity thresholds vary over x for a given γ. For example, the closer a pixel is to the center of the scan, known as nadir (x = 0), the greater its intensity must be to be detected as a bright [7], and the lower its intensity must be to be detected as a shadow. It is interesting to note that the two threshold curves do not diverge from their respective asymptotes (i_{min} and i_{max}) at the same rate as they approach nadir. This is by design, because shadows are more detectable than brights in SSI [8] – [11]. In other words, a single shadow threshold value (i_{min}) suffices for more values of x than a single bright threshold value (i_{max}).

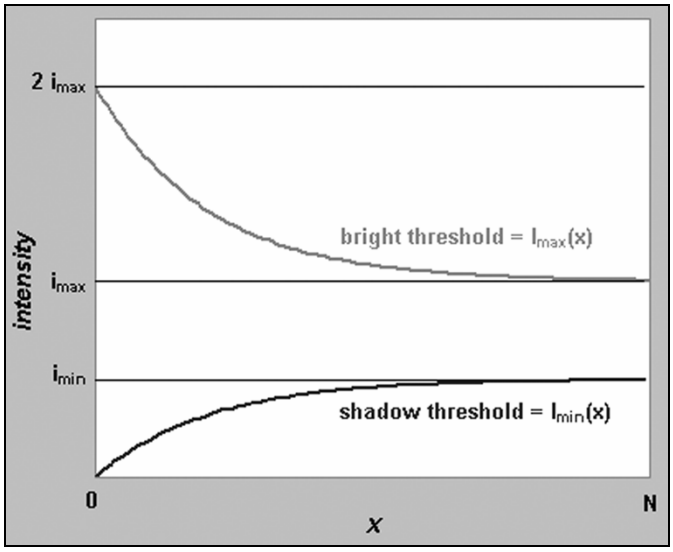

Fig. 3. Intensity thresholds for brights and shadows.

D. Circular Lookup Table

Finally, the bright and shadow geospatial bitmaps are examined from the edges of the scan lines toward the center (nadir) to detect runs of shadows followed by runs of brights. A circular lookup table is created to "window" several scan lines at a time. This lookup table is populated with positions and run-lengths of shadows and brights. The window information is used to determine if a series of scan-line detections comprise an object. Shadow length is one component in determining the object's height, which is used to help determine whether the object is mine-like. The authors theorized that height also could be used to automatically estimate seafloor roughness (or bottom relief).

III. Automated Roughness Algorithm

NRL developed an automated algorithm to estimate seafloor roughness from SSI, which is based on the clutter detection algorithm described above. In the new roughness algorithm, the authors used sensor altitude above the seafloor, distance of the shadow from nadir, length of the shadow (determined by the clutter detection algorithm) and sonar resolution to estimate roughness. The resulting roughness maps use shaded or outlined polygons to delineate smooth and rough areas.

The algorithm was first tested on two geographic regions (labeled I and II) and compared with manual roughness estimated by expert analysts at NAVOCEANO. The algorithm detected bottom object locations for each region, clustered them into polygons, and categorized the regions as relatively smooth or rough.

IV. Test Results

Fig.s 4 and 5 show the manual polygons (white outlines) overlaid on results of the roughness algorithm (light-gray-filled polygons) for Regions I and II, respectively. The percentage of agreement between manual and automated polygons is approximately 60% for Region I and 84% for Region II. This is equivalent to %correct for the automated method, assuming the manual method is ground-truth). Importantly, both the manual and automated methods clearly indicate a smooth "lane" running through the center of the SSI in Region I. During mine warfare operations, bottom roughness is one of the components considered when choosing which navigation lanes to clear of mines, since it is easier to clear a smooth seafloor than a rough one.

Another test, over a third region in 2006, resulted in 87% agreement, shown in Fig. 6. Table 1 shows how the authors calculated percent agreement.

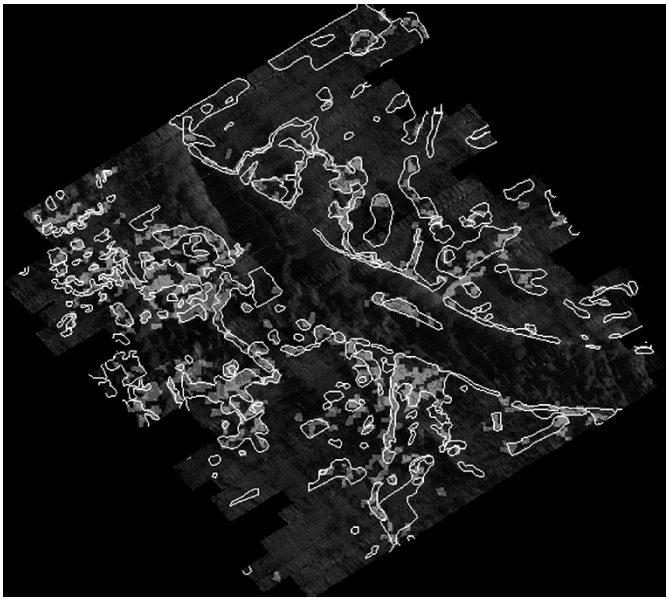

Fig. 4. Roughness estimations for Region I: determined manually (white outlines) and with the NRL Automated Roughness Algorithm (light gray filled regions). The percentage of agreement between manual and automated roughness estimations is 60%.

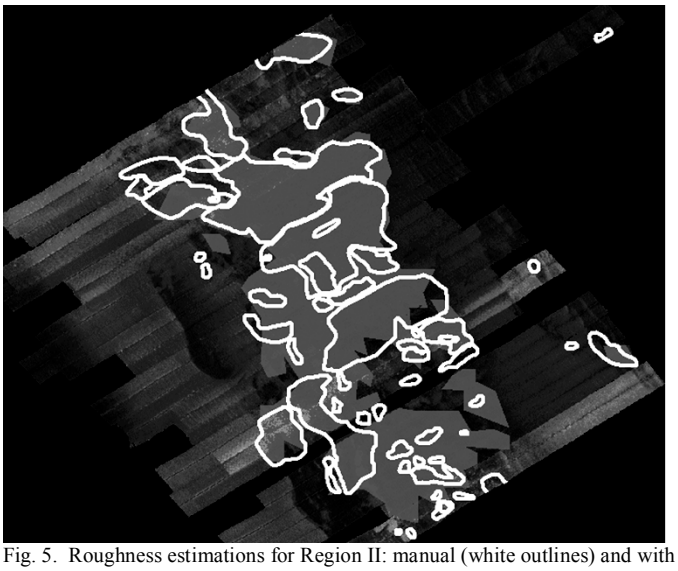

Fig. 5. Roughness estimations for Region II: manual (white outlines) and with the NRL Automated Roughness Algorithm (light gray filled regions). The percentage of agreement between manual and automated roughness estimations is 84%.

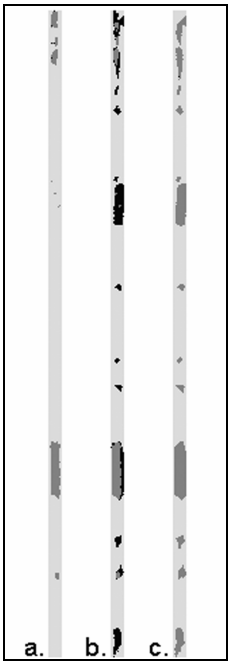

Fig. 6. Roughness estimations for Region III: a) manual estimation only; b) manual and automated combined; c) automated estimation only. Light gray areas were judged to be smooth, medium and dark gray areas rough. Table I provides additional explanation.

TABLE I
CALCULATING %CORRECT FOR RESULTS
OF AUTOMATED ROUGHNESS ALGORITHM

	#pixels	%image	Description
¾	3822	79.3%	Correct (smooth)
¾	349	7.2%	Correct (rough)
		86.5%	Total correct
¾	649	13.5%	Incorrect: false alarms (falsely categorized smooth areas as rough)
	0	0.0%	Incorrect: missed detections (falsely categorized rough areas as smooth)
		13.5%	Total incorrect (false alarms only)

ACKNOWLEDGMENT

The authors thank Mr. James Hammack and Mr. Chuck Martin of NAVOCEANO for their technical support during this project.

REFERENCES

[1] B. Reed, "Data, Data Everywhere and Nary a Bit to Drop," Abstract for the *Shallow Survey 2001 Conference*, Sidney, Australia, p. 1, 2001.

[2] D. Cronin, M. Broadus, B. Reed, S. Byrne, W. Simmons, and L. Gee, "Hydrographic Work Flow – From Planning to Products," Proc. of the *U.S. Hydro 2003 Conference*, March 24-27, Biloxi, Mississippi, pp. 1-13, 2003.

[3] F. Winsberg, M. Elkin, J. Macy, V. Bordaz, W. Weymouth, "Detection of Radiographic Abnormalities in Mammograms by Means of Optical Scanning and Computer Analysis," *Radiology 1967*, vol. 89, pp. 211-215, 1967.

[4] L. V. Ackerman and E. E. Gose, "Breast Lesion Classification by Computer and Xeroradiograph," *Cancer*, vol. 3, no. 4, October, pp. 1025-1035, 1972.

[5] M. L. Giger, *CE: Mammography 4: Update on Computer-Aided Diagnosis in Mammography Handout*, AAPM meeting, Salt Lake City, Utah, pp. 1-26, 2001.

[6] M. Gendron, P. Wischow, M. Trenchard, M. Lohrenz, L. Riedlinger, and M. Mehaffey, *Moving Map Composer*, Naval Research Laboratory, U.S. Patent No. 6,218,965, 2001.

[7] P. Blondel and B Murton, *Handbook of Seafloor Sonar Imagery*, New York, John Wiley & Sons, pp. 23-46, 1997.

[8] M. C. Mignotte, C. Collet, P. Perez and P. Bouthemy, "Markov Random Field and Fuzzy Logic Modeling in Sonar Imagery: Application to the Classification of Underwater Floor," *Computer Vision and image Understanding*, vol. 79, no. 1, pp. 4-24, 2000.

[9] M. C. Mignotte, C. Collet, P. Perez and P. Bouthemy, "Sonar Image Segmentation Using an Unsupervised Hierarchical MRF Model," *IEEE Transactions on Image Processing*, vol. 9, no. 7, pp. 1216-1231, 2000.

[10] S. Reed, E. Dura, D. M. Lane, Y. J. Petillot, "Extraction and Classification of Objects from Sidescan Sonar Bell," *IEEE Workshop on Nonlinear and Non-Gaussian Signal Processing*, July 8-9, pp. 1-2, 2002.

[11] S. Reed, Y. Petillot, J. Bell, "An Automatic Approach to the Detection and Extraction of Mine Features in Sidescan Sonar," *IEEE Journal of Oceanic Engineering*, vol. 28, no. 1, pp. 90-105, 2003.